Optimal angle bounds for Steiner triangulations of polygons

Christopher J. Bishop *

Abstract

For any simple polygon P we compute the optimal upper and lower angle bounds for triangulating P with Steiner points, and show that these bounds can be attained (except in one special case). The sharp angle bounds for an N-gon are computable in time $O(N)$, even though the number of triangles needed to attain these bounds has no bound in terms of N alone. In general, the sharp upper and lower bounds cannot both be attained by a single triangulation, although this does happen in some cases. For example, we show that any polygon with minimal interior angle θ has a triangulation with all angles in the interval $I = [\theta, 90^\circ - \min(36^\circ, \theta)/2]$, and for $\theta \le 36^\circ$ both bounds are best possible. Surprisingly, we prove the optimal angle bounds for polygonal triangulations are the same as for triangular dissections. The proof of this verifies, in a stronger form, a 1984 conjecture of Gerver.

1 Statement of results

This is an announcement of results that are proven in full in [8]. Some proofs will sketched here, but various details, especially involving estimates for conformal or quasiconformal mappings are left for [8].

It is a problem of long-standing theoretical and practical interest to triangulate a polygon with the best possible bounds on the angles used. For example, the constrained Delaunay triangulation famously maximizes the minimal angle if no additional vertices (called Steiner points) are allowed [23], [24], and algorithms for minimizing the maximum angle (again without Steiner points) are given in [2] and [15]. Here we solve the analogous problems when Steiner points are permitted.

In this case, Burago and Zalgaller [9] proved in 1960 that every planar polygon P has an acute triangulation (all angles $< 90^\circ$). This is the sharpest bound that holds for all polygons, but what are the optimal upper and lower angle bounds for triangulating a given polygon P with Steiner points? Are these bounds attained or can they only be approximated? Can both bounds be attained simultaneously? How regular are the corresponding triangulations? How do the angle bounds for triangulations differ from those for dissections? Using ideas involving conformal and quasiconformal mappings, we shall answer each of these questions. However, the emphasis of our results is on computing the optimal angle bounds; finding efficient triangulations that attain these bounds remains an interesting open question.

We start with some notation. Suppose $\mathcal{T}$ is a triangulation of P. Let V_P be the vertex set of P, $V_{\mathcal{T}}$ the vertex set of $\mathcal{T}$, $\partial\mathcal{T} = V_{\mathcal{T}} \cap P$ the **boundary vertices** of $\mathcal{T}$, and let $\text{int}(\mathcal{T}) = V_{\mathcal{T}} \setminus \partial\mathcal{T}$ denote the **interior vertices**. Label each $v \in V_{\mathcal{T}}$ with the number, $L(v)$, of triangles in $\mathcal{T}$ that have v as a vertex. For $v \in \partial\mathcal{T}$, we define its **discrete curvature** as $\kappa(v) = 3 - L(v)$, and for an interior vertex we set $\kappa(v) = 6 - L(v)$. Using these definitions, Euler's formula applied to a triangulation can be rewritten to look like the Gauss-Bonnet formula:

$$\sum_{v \in \text{int}(\mathcal{T})} \kappa(v) = 6 - \sum_{v \in \partial\mathcal{T}} \kappa(v). \tag{1.1}$$

We define this common value to be $\kappa(\mathcal{T})$, the **curvature of the triangulation**.

For $\phi > 0$, a **ϕ-triangulation** of P is one with all angles at most ϕ. For $\phi \in [60^\circ, 90^\circ]$ define the interval $I(\phi) = [180 - 2\phi, \phi]$. Any ϕ-triangulation must have all of its angles in $I(\phi)$ (since the sum of all three angles is 180°, if two are $\le \phi$, the third is $\ge 180^\circ - 2\phi$). Let $|V_P|$ be the number of vertices in P, and for $v \in V_P$, let θ_v denote the interior angle of P at v. A labeling $L : V_P \to \mathbb{N} = \{1, 2, \ldots\}$ is called **ϕ-admissible** if $\theta_v \in L(v) \cdot I(\phi)$

*The author is partially supported by NSF Grant DMS 1906259.

for every $v \in V_P$. The **curvature of a labeling** L is defined as

$$\kappa(L) = \sum_{v \in V_P} L(v) - (3|V_P| - 6) = 6 - \sum_{v \in V_P} (3 - L(v)).$$

If a labeling L of V_P comes from a ϕ-triangulation $\mathcal{T}$ of P with $\phi < 90°$, then it is automatically ϕ-admissible and satisfies $\kappa(L) \le \kappa(\mathcal{T})$, since vertices of $\partial\mathcal{T} \setminus V_P$ must have degree ≥ 3. If $\phi < 72°$ then $\text{int}(\mathcal{T})$ has no vertices of degree ≤ 5, so (1.1) implies $\kappa(L) \le \kappa(\mathcal{T}) \le 0$. See Figure 1. Similarly, if $\phi < \frac{5}{7} \cdot 90° \approx 64.2857°$ then every vertex in $\text{int}(\mathcal{T})$ has degree 6 and every vertex in $\partial\mathcal{T} \setminus V_P$ has degree 3, so $\kappa(L) = \kappa(\mathcal{T}) = 0$. Remarkably, these elementary necessary conditions are also sufficient.

THEOREM 1.1. *For $60° < \phi \le 90°$, a polygon P has a ϕ-triangulation iff*

1. *$72° \le \phi < 90°$ and there is some ϕ-admissible labeling L of V_P,*
2. *$\frac{5}{7} \cdot 90° \le \phi < 72°$, and there is a ϕ-admissible labeling with $\kappa(L) \le 0$,*
3. *$60° < \phi < \frac{5}{7} \cdot 90°$, and there is a ϕ-admissible labeling with $\kappa(L) = 0$.*

For $60° < \phi < 90°$ define $\mathcal{K}(\phi)$ be the set of possible values of $\kappa(L)$ over all ϕ-admissible labelings of V_P; we set $\mathcal{K}(\phi) = \infty$ if there is no admissible labeling. Note that $\mathcal{K}(\phi)$ is either ∞ or a non-empty interval of integers. Hence $\mathcal{K}(\phi)$ has a unique closest element to 0, denoted $\kappa(\phi)$ (possibly 0 or ∞). The three conditions in Theorem 1.1 can be restated as $\kappa(\phi) < \infty$, $\kappa(\phi) \le 0$ and $\kappa(\phi) = 0$ respectively. (We should write $\mathcal{K}(\phi, P), \kappa(\phi, P)$, since these quantities also depend on P, but in this paper P is usually fixed and clear from context.)

Theorem 1.1 fails for $\phi = 60°$: Figure 1 shows that a polygon can satisfy $\kappa(60°) = 0$, but have no equilateral triangulation. However, if $\kappa(60°) = 0$, then P can be triangulated using only angles $\le 60° + \epsilon$ for any $\epsilon > 0$; see Lemma 3.4. This is the only case where the optimal bound need not be attained by any triangulation. Note that $\kappa(60°) = 0$ if and only if P is a $60°$**-polygon**, i.e., all angles are multiples of $60°$. Such a polygon has an equilateral triangulation iff all of its edge lengths are integer multiples of a single value.

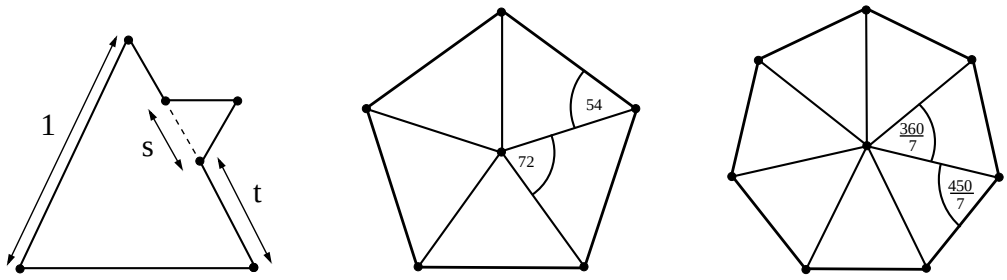

Figure 1: The left polygon satisfies $\kappa(60°) = 0$, but has no equilateral triangulation unless both s and t are rational. The other pictures show where the special angles in Theorem 1.1 come from: these angles are forced by interior vertices of degree five or seven.

For a simple polygon P, and let $\theta_{\min}$ and $\theta_{\max}$ denote the minimum and maximum interior angles of P and define $\Phi(P)$ to be the infimum of ϕ such that P has a ϕ-triangulation. Theorem 1.1 makes it easy to compute $\Phi(P)$. To illustrate this, we list a few corollaries of the result and its proof. The proofs may be found in [8].

COROLLARY 1.1. *$\Phi(P)$ can be computed in time $O(|V_P|)$.*

COROLLARY 1.2. *For any polygon, $\Phi(P) \le 90° - \min(\theta_{\min}, 36°)/2$. If $\theta_{\min} \le 36°$, then $\Phi(P) = 90° - \frac{1}{2}\theta_{\min}$ and P has a triangulation $\mathcal{T}$ with all angles in $[\theta_{\min}, 90° - \theta_{\min}/2]$.*

COROLLARY 1.3. *For the regular N-gon P_N, $\Phi(P_N) = 72°$ except when $N = 3, 6, 7, 8, 9$; then $\Phi(P_N) = 60°$, $60°$, $\frac{5}{7} \cdot 90°$, $67.5°$, and $70°$ respectively.*

A **triangular dissection** covers P and its interior by finitely many closed triangles with disjoint interiors. The edges of adjacent triangles need not match up exactly; if they do, then we have a triangulation. See Figure 2. A **ϕ-dissection** is a triangular dissection with maximum angle $\leq \phi$. In 1984 Gerver [18] showed that the conditions in Theorem 1.1 are necessary if P has a $(\phi+\epsilon)$-dissection for every $\epsilon > 0$, and he conjectured that they were sufficient for a ϕ-dissection to exist if $\phi > 60°$.

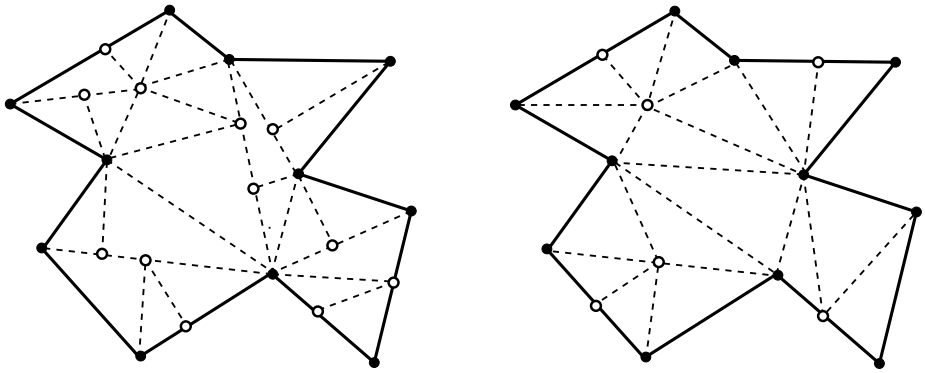

Figure 2: On the left is a dissection of a polygon and on the right a triangulation. The white dots the Steiner points. Despite triangulations being more restrictive than dissections, the optimal upper angle bounds are the same for both types of decomposition.

COROLLARY 1.4. *For a polygon P and $\phi \in (60°, 90°]$, the following are equivalent:*

1. *For every $\epsilon > 0$, P has a $(\phi+\epsilon)$-dissection,*
2. *P has a ϕ-dissection,*
3. *P has a ϕ-triangulation.*

This is surprising (at least to the author). Since dissections satisfy much less stringent conditions than triangulations do, one might expect a gap between the best possible angle bounds in these two cases, but such a gap does not occur. Given a ϕ-dissection, can one obtain a ϕ-triangulation from it, e.g., as a refinement?

The conditions in Theorem 1.1 only depend on the set of angles of P, not on their ordering around P, nor on the side lengths of P. This solves Problem C7 of [11].

COROLLARY 1.5. *If $\phi > 60°$ and P, P' are N-gons with the same set of angles (possibly in different orders around the boundary) then P has a ϕ-triangulation (or a ϕ-dissection) if and only if P' does.*

As noted earlier, the Delaunay triangulation maximizes the minimal angle needed to triangulate a point set without Steiner points (with Steiner points, angles arbitrarily close to 60° can be achieved for point sets). The constrained Delaunay triangulation does the same for polygonal triangulations without Steiner points (see [23], [24]), and an algorithm using only interior Steiner points is presented in [28]. The methods of this paper can be used to maximize the minimum angle for triangulating a polygon P with arbitrary Steiner points. To see how this works, suppose $0 < \phi < 60°$ and define $\widetilde{I}(\phi) = [\phi, 180° - 2\phi]$; similar to the argument given for $I(\phi)$, any triangle having smallest angle ϕ must have all its angles inside $\widetilde{I}(\phi)$. Define a labeling L to be ϕ-lower-admissible if $\theta_v \in L(v) \cdot \widetilde{I}(\phi)$ where θ_v is the angle of P at $v \in V_P$. The curvature $\kappa(L)$ is defined just as before, and $\widetilde{\mathcal{K}}(\phi)$ is the set of curvatures of ϕ-lower-admissible labelings. Also as before, $\widetilde{\kappa}(\phi)$ is the element of this set closest to 0 (equal to ∞ if no ϕ-lower-admissible labeling exists). A ϕ-lower-triangulation is a triangulation with all angles $\geq \phi$. We define $\widetilde{\Phi}(P)$ to be the supremum of ϕ so that P has a ϕ-lower-triangulation.

THEOREM 1.2. *For $0 < \phi < 60°$, a polygon P has a ϕ-lower-triangulation iff*

1. *$0 < \phi \leq \frac{1}{7} \cdot 360° \approx 51.4286°$ and $\widetilde{\kappa}(\phi) < \infty$,*

2. $\frac{1}{7} \cdot 360^\circ < \phi \leq 54^\circ$, *and* $\widetilde{\kappa}(\phi) \geq 0$,

3. $54^\circ < \phi < 60^\circ$, *and* $\widetilde{\kappa}(\phi) = 0$.

As before, there are a variety of consequences that follow; these are proven in [8].

COROLLARY 1.6. *$\widetilde{\Phi}(P)$ can be computed in time $O(|V_P|)$.*

COROLLARY 1.7. *If P has a ϕ-lower-triangulation then it also has an acute ϕ-lower-triangulation.*

COROLLARY 1.8. *If $\theta_{\min} \leq 45^\circ$, then $\widetilde{\Phi}(P) = \theta_{\min}$.*

Comparing Corollaries 1.2 and 1.8, we see that if P is a polygon with $\theta_{\min} = 45^\circ$, then $\Phi(P) \leq 72^\circ$ and $\widetilde{\Phi}(P) \geq 45^\circ$. If P has at least one angle $\theta \in (72^\circ, 90^\circ)$, then any triangulation of P that attains the optimal upper bound $\Phi(P)$ must subdivide θ and hence has an angle strictly less than $45^\circ \leq \widetilde{\Phi}(\phi)$.

COROLLARY 1.9. *There exist polygons so that any triangulation attaining the optimal upper angle bound $\Phi(P)$, does not achieve the optimal lower angle bound $\widetilde{\Phi}(P)$.*

The idea behind both Theorems 1.1 and 1.2 is to associate to each polygon P a model polygon P', and then to transfer a nearly equilateral triangulation from P' to P using a conformal map. We map the triangulation vertices from P' to P and connect them by segments in P; we call these the "pushed forward" triangles (conformal images of the triangles themselves would have curved sides). A simple example is shown in Figure 3. The labeling shown in Figure 3 is 72°-admissible and has curvature 0, so $\kappa(72^\circ) = 0$. Moreover, the reader can check that $\kappa(\phi) > 0$ for $\phi < 72^\circ$, hence $\Phi(P) = 72^\circ$. As the mesh in Figure 3 gets finer, the largest angle tends to 72°, and we will show later that this limiting bound can be attained by modifying a sufficiently fine triangulation near the vertices (see Lemma 3.7).

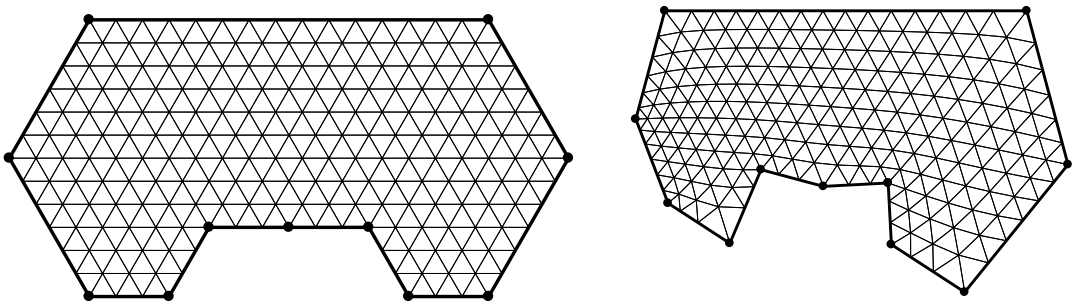

Figure 3: An equilateral triangulation of P' (left) and its conformal image P (angles: 270°, 126°, 96°, 126°, 105°, 105°, 144°, 144°, 80°, 262°, 162°). The maximum angle used here is $\approx 73.5205^\circ$ and approaches 72° as the mesh gets finer; 72° is sharp by Theorem 1.1 and can be attained by modifying a sufficiently fine triangulation near the vertices.

We want P' to have a (nearly) equilateral triangulation, so we will assume it is a 60°-polygon. Note that any equilateral triangulation of P' has all interior vertices of degree six. The angle of P' at the vertex corresponding to $v \in V_P$ is given by $60^\circ \cdot L(v)$, where L is a labeling of V_P. Since the angles of P' sum to $(|V_P| - 2) \cdot 180^\circ$, a short calculation shows that we must have $\kappa(L) = 0$. Given such a labeling of V_P, we will use the Schwarz-Christoffel formula to define P' and f. If we transfer a sufficiently fine and nearly equilateral triangulation from P' to P using f, the image will be close to a ϕ-triangulation of P if the labeling L is ϕ-admissible. Thus to start the construction it seems that we need a ϕ-admissible labeling of P with zero curvature.

However, such a labeling need not exist. For example, suppose P is a pentagon with five equal angles of 108°. Theorem 1.1 (in particular, Corollaries 1.3 and 1.5) implies that $\Phi(P) = 72^\circ$. However, the only 72°-admissible labels for a 108°-vertex are $\{2, 3\}$, so $\mathcal{K}(\phi) = \{1, \ldots, 6\}$ and so $\kappa(\phi) = 1 > 0$. This holds even if we add extra

180°-vertices to P (their possible labels are $\{3, 4, 5\}$). Therefore, any 72°-triangulation of P has positive curvature and thus at least one interior vertex of degree five (degree ≤ 4 implies an angle $\geq 90°$).

How can such a triangulation be a conformal image of a triangulation of P' that only has interior vertices of degree six? The answer is that we can choose f to conformally map the interior of P' into a subdomain of P obtained by cutting a slit in P. Two adjacent edges of P' are mapped to the two sides of the slit, and some boundary vertices of P' become interior vertices of P, thus the topology of the triangulation changes. See Figure 4. In general, up to $|\kappa(\Phi(P))|$ slits are used, introducing vertices of either degree five ($\kappa > 0$) or degree seven ($\kappa < 0$).

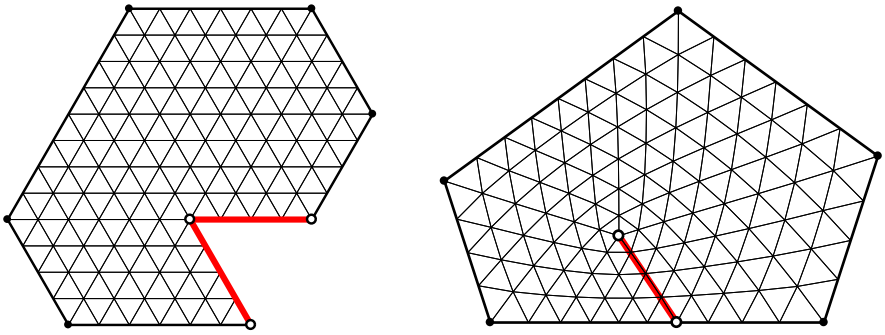

Figure 4: The edges adjacent to the 300°-vertex of P' are mapped to the two sides of the slit inside P. An interior vertex v of degree 5 is created. The slit is slightly curved to make the triangles on either side match up, although this is not easily visible (the actual slit lies slightly above the chord between its endpoints).

This scheme encounters a number of difficulties, that we will overcome using ideas from complex function theory. We list a few here, giving details later.

• **Conformal welding:** When we map boundary edges of P' to a slit in P, the images of certain boundary triangles in P' must match up across the slit in P, so that the image is a triangulation and not a dissection. This is only possible if the shape of the slit is carefully chosen so that arclength on each boundary segment maps to the same measure on the slit, i.e., we need $f(z) = f(w) \Rightarrow |f'(z)| = |f'(w)|$. This is a special case of a conformal welding problem, e.g., [6], [20], [30], and in our case it can be solved explicitly using power maps.

• **Riemann surfaces:** In cases where we introduce an interior vertex of degree seven, P' will need to have a boundary vertex of degree seven, i.e., P' has interior angle 420° at some vertex. Thus we necessarily consider "polygons" P' that are actually Riemann surfaces and not planar regions. See Figure 5.

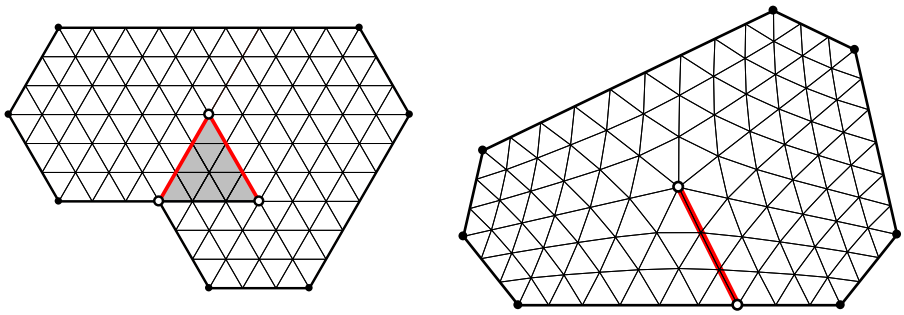

Figure 5: We triangulate an equal-angle heptagon using a Riemann surface with a 420°-vertex to insert a degree 7 vertex into the triangulation. The self-overlapping part of the surface is shaded.

• **Distortion estimates:** A conformal map f preserves interior angles infinitesimally, but to control our triangulation angles we shall need angle distortion estimates at positive scales, with bounds depending on the size of the triangle, its distance to the nearest vertex, and the ratio of the corresponding angles in P and P' at that vertex. Here we make use of the classical distortion theorems for conformal maps.

• **Quasiconformal mappings:** Given two triangulations of a region arising from different, but close, conformal maps, we merge the triangulations by using a partition of unity to interpolate from one conformal map to the other. The result is a quasiconformal map, and we shall use standard estimates on the angle distortion of such maps to control the angles of the interpolated triangulations. We also use such estimates to prove that any 60°-polygon has a nearly equilateral triangulation.

In 1992 Edelsbrunner, Tan and Waupotitsch [15] gave a $O(N^2 \log N)$ algorithm for minimizing the maximum angle of a polygonal triangulation without using Steiner points (their result has not been improved, so far as I know). Thus Corollary 1.1 says that it is actually faster to compute the optimal angle bound when allowing Steiner points. However a triangulation achieving the optimal bound might not be computable in polynomial time (see the remarks below), and this paper does not address the question of finding efficient triangulations attaining the optimal bounds. See the last section of [8] for some ideas on how this might be done.

Finding triangulations with good angle bounds has a long history and many applications, e.g, see [7] or [38] for lists of algorithms, such as the finite element method, that work better with well formed meshes. Corollary 1.2 gives an explicit bound for the acute triangulation theorem of Burago and Zalgaller [9] mentioned earlier. Their result was an element of their polyhedral version of the Nash embedding theorem, but it long remained unknown in the computational geometry literature. The first reference to it that I am aware of is [21] in 2004. In 1988 Baker, Grosse and Rafferty [1] independently proved that every polygon has a non-obtuse triangulation (all angles $\leq 90°$). This led to a large literature on algorithms for finding triangulations in various settings with guaranteed angle bounds, e.g., [3], [4], [5], [7], [14], [17], [22], [25], [27], [31]. For a recent survey, see Chapter 29 of [19]. In 2002 Maehara [26], showed every non-obtuse triangulation can be converted to an acute one (with a comparable number of triangles), giving an alternate proof of the Burago-Zalgaller result (see also Yuan's paper [37]). A simpler approach was given by Saraf in [32].

Despite much effort devoted to finding triangulations with good geometry and optimal complexity, finding triangulations with optimal geometry has attracted less attention, at least when Steiner points are allowed. One case that has been considered is triangulating the square with optimal angles, a problem discussed by Gerver in [18] and by Eppstein in [16]. One possible reason that Theorem 1.1 has been overlooked is the close connection to conformal mappings; at least it is difficult to see how our proof could have been discovered using purely discrete geometric ideas.

Another reason may be the traditional focus on complexity. If the size of the triangulation is bounded by a function of $N = |V_P|$, independent of the geometry, then 90° is the best possible upper angle bound. For example, if a $1 \times R$ rectangle with $R \gg 1$ is triangulated by $O(1)$ triangles, then there must be a small angle $\theta = O(1/R)$, and hence some angle $\geq 90° - \theta/2$. Thus the complexity of an angle-optimal triangulation of an N-gon is not polynomial in N. Even so, the sharp angle bounds proven here are fast to compute and provide a benchmark against which other triangulation methods can be compared.

Section 2 gives an overview of the proof Theorem 1.1, and later sections provide further details, assuming various estimates related to conformal and quasiconformal mappings that are proven in [8]. That paper also contains the proofs of the corollaries stated in this section and a variety of other consequences of Theorems 1.1 and 1.2. I thank Joe Mitchell and Herbert Edelsbrunner for their encouraging and helpful comments on an earlier version of this paper. I also thank the anonymous referees who read the paper for SODA 2022 and provided numerous suggestions. Several figures are drawn using Toby Driscoll's SC-Toolbox package for MATLAB [12], an improved version of an earlier algorithm of Nick Trefethen [36] for computing Schwarz-Christoffel maps. I thank Toby for his assistance with the toolbox.

2 Overview of the proof

The basic idea is quite simple: we introduce a class of polygons that have "nearly equilateral" triangulations (all angles close to 60°) and use conformal maps to transfer these triangulations to general polygons.

We will say that a simple polygon is an **equilateral grid-polygon** if its edges are contained in a grid of the plane consisting of congruent equilateral triangles, and its vertices are vertices of the grid. These are exactly the simple polygons that have a triangulation by equilateral triangles. See Figure 6.

It will be convenient to enlarge this class to the class of **60°-polygons**, whose interior angles are all multiples of 60°. We will say that a polygon P has **nearly equilateral triangulations** if for any $\epsilon > 0$ it has a triangulation with all angles in $[60° - \epsilon, 60° + \epsilon]$ and that each vertex of P has a neighborhood in which the triangulation elements are actually equilateral (this is needed to attain the desired angle bounds, instead of just approximating

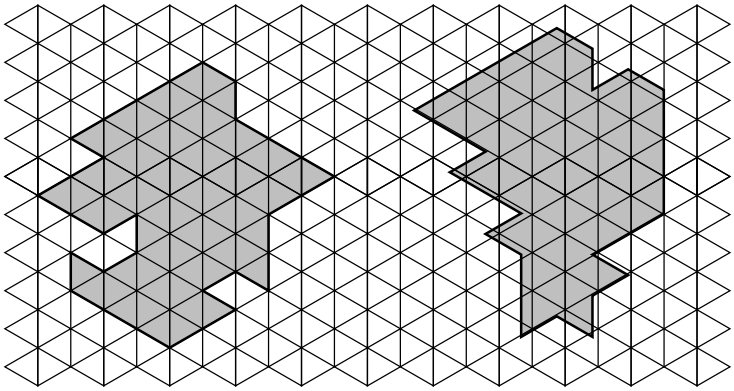

Figure 6: On the left is a equilateral-grid polygon, and on the right is a 60°-polygon.

them). We will prove that every 60°-polygon has nearly equilateral triangulations; see Lemma 3.4. This lemma includes 60°**-surfaces**, i.e., simply connected Riemann surfaces R obtained by identifying 60°-polygons along matching edges. The boundary of R projects into the plane, possibly with self-intersections. Such surfaces can arise as Schwarz-Christoffel images of the disk (see Section 6) when all the angles are multiples of 60°, but the map is not globally 1-to-1.

Suppose $f : \Omega' \to \Omega$ is a conformal mapping between the interiors of two polygons P' and P, and that f induces a bijection between vertices of P' and vertices of P. (Below, we will often use P to refer to both the boundary curve and the interior domain, instead of using Ω for the latter; the meaning should always be clear from context.) Then f will only slightly perturb the angles of sufficiently small triangles in Ω', unless they are near vertices of P' (see Corollary 3.1). If v' is a vertex of P' with angle ψ that maps to a vertex v of P with angle θ, then any small triangle close enough to v' will have its interior angles distorted by at most θ/ψ (Lemma 3.6).

The triangulations we construct will have all their angles between 36° and 72°, except for some triangles near vertices of P that have angle less than 36°. Larger angles of P will be subdivided by the triangulation to give new angles that are all in the interval $[36°, 72°]$, and these sub-angles should each map to 60° under the conformal map from P to P'. In order to have this work out correctly, we need an angle θ in P to correspond to an angle $\psi = L(v) \cdot 60°$ in P' that satisfies

$$\frac{3}{5}\psi \le \theta \le \frac{6}{5}\psi. \tag{2.2}$$

The restrictions imposed by (2.2) are summarized by Table 1 and Figure 7. For example, if P has a vertex v with interior angle $\theta = 135°$ the corresponding vertex v' in the 60°-polygon P' must have angle either 120° or 180°. Any other choice means that the triangles containing v' in the nearly equilateral triangulation of P' map to triangles with angles either less than 36° or larger than 72°.

θ range	allowable ψ
0–72	60
72–108	120
108–144	120, 180
144–180	180, 240
180–216	180,240, 300
216–288	240, 300, 360
288–360	300, 360

Table 1: Given an angle θ of P, this table gives the possible corresponding ψ's in P' needed to attain $\Phi(P) \le 72°$. Note that angles $\le 36°$ in P will always give angles $\ge 72°$ in the triangulation.

Figure 7 plots $\bigcup_k k \cdot I(\phi)$ vertically above each value of ϕ. The result is a union of shaded triangles. P has a ϕ-admissible labeling if and only if all its angles lie in the intersection of the shaded region and the vertical line

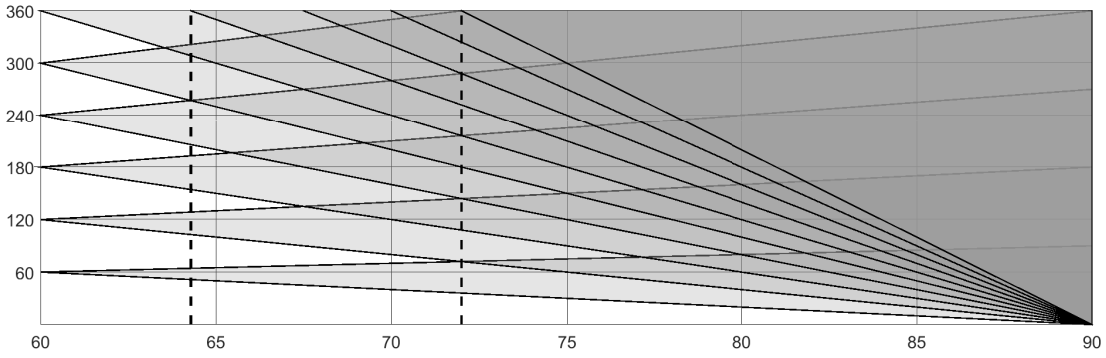

Figure 7: P has a ϕ-admissible labeling iff all its angles lie in the union of shaded triangles, on the vertical line through ϕ. The dashed vertical lines indicate where the transitions occur in Theorem 1.1, i.e., $\phi = \frac{5}{7} \cdot 90°$, and $\phi = 72°$.

through ϕ. For $72° \le \phi \le 90°$, $\cup_k k \cdot I(\phi) = [180° - 2\phi, \phi]$ so this condition only depends on the size of $\theta_{\min}$, and is equivalent to having a ϕ-triangulation. For $\phi < 72°$, having a ϕ-triangulation requires other conditions as well, involving which triangles the angles of P lie in.

Unfortunately, there are some polygons P whose vertices cannot be put into 1-1 correspondence with the vertices of a 60°-polygon so that they satisfy the restrictions in Table 1 and Figure 7. In general, the interior angles $\{\theta_1, \ldots, \theta_N\}$ of an N-gon must satisfy $\sum_k \theta_k = (N-2)180°$. When we assign image angle values $\{\psi_1, \ldots, \psi_N\}$ using (2.2) or Table 1, we need to have $\sum_k \psi_k = (N-2)180°$, but this is sometimes impossible. For example, if P is a square, then each of its four 90° angles would have to be assigned angle 120° in P', giving an angle sum $480° > 360°$. We can "fix" the angle discrepancy by adding extra vertices to the edges of P.

First suppose $\sum_k \psi_k < \sum_k \theta_k$. We add a new vertex v of angle 180° in an edge of P, and assign the corresponding vertex v' in P' the angle $240° \le \frac{6}{5} \cdot 180°$. See Figure 8. Doing this increases the angle sum $\sum \theta_k$ by 180° but increases the angle sum $\sum \psi_k$ by 240°, decreasing the gap between them by 60°. Doing this several times we can clearly make the two sums match, as desired. Four equilateral triangles in P' touch v', and they are mapped to four triangles in P touching v. they have angle 45° at v and the opposite angles are approximately 67.5° (some distortion may occur). Hence using this method can only give ϕ-triangulations with $\phi \ge 67.5°$. This is adequate to prove Case 1 of Theorem 1.1 but a more elaborate construction is needed to prove Cases 2 and 3.

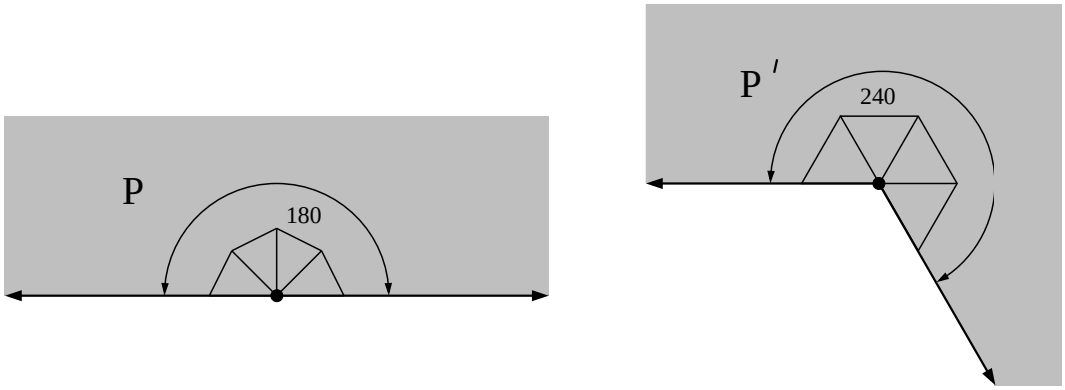

Figure 8: Our first trick for increasing the ψ-sum relative to the θ-sum is to pair a 180°-vertex in P with a 240°-vertex in P'. The conformal map locally looks like $z^{3/4}$, and maps a 60° sub-angle to 45°. A triangle containing a 45° angle also contains an angle ≥ 67.5.

In Case 2 of Theorem 1.1 we want to get the angle 67.5° down to $\frac{5}{7} \cdot 90° \approx 64.2857$. We will do this by using a triangulation of a slit half-plane based on transferring an equilateral triangulation from a polygonal Riemann

surface that has a 420° angle in its boundary. The idea is shown in Figure 9; the details will be given in Section 5. The Riemann surface R is built by attaching two planar domains as shown on the left side of Figure 16. R has a 1-1 projection onto a sector of angle 240°, except for the darker triangle where it is 2-1. Traversing the boundary, we encounter angles 60°, 420° and 120°. The 420°-vertex belongs to seven triangles in R and will map to a degree seven interior vertex in the final triangulation.

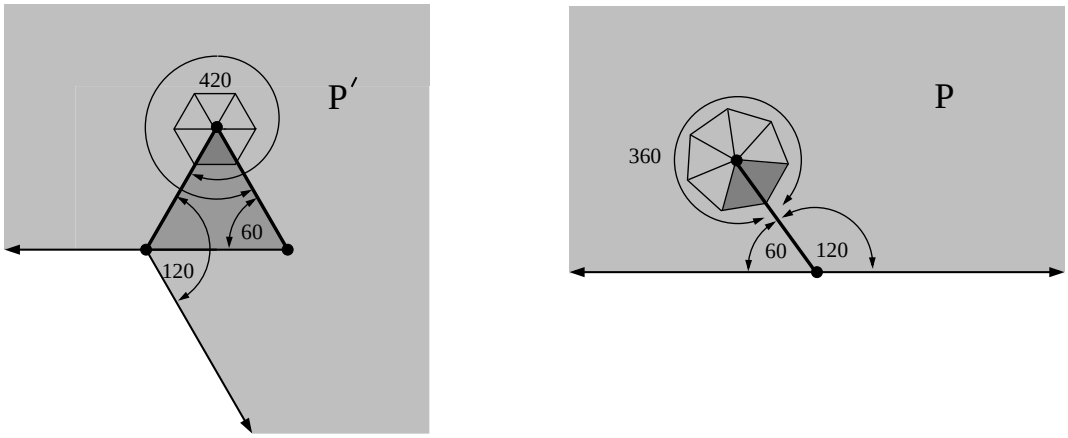

Figure 9: We cut a slit in the upper half-plane at angle 60°. This models a neighborhood of a 180°-vertex on the boundary of P. The angles we observe tracing the outline of the slit are: 60°, 360° and 120°. The triangulation near this slit will correspond to an equilateral triangulation of a Riemann surface R with angles 60°, 420° and 120°, pictured at right. R is a 1-1 cover of a 240°-sector, except for the darker triangle where it is 2-1.

The two segments adjacent to the 420°-vertex are mapped to a slit in P where the angles are 60°, 180° and 120°. The worst distortion comes from mapping the 420°-vertex in P' to the 360°-vertex in P (the tip of a slit). Locally the map looks like $z^{6/7}$, that maps each 60° sub-angle to $\frac{6}{7} \cdot 60° = \frac{4}{7} \cdot 90° \approx 51.4286$. A triangle with this angle must also contain an angle $\geq \frac{5}{7} \cdot 90° \approx 64.2857$, which is where this angle in Theorem 1.1 comes from. Note that the two finite boundary segments of R are both mapped to the slit in P, so triangulation edges along these two sides of R must map to matching edges along the slit. This requires that the conformal map sends the length measures on the two segments to the same measure on the slit (but not necessarily length measure). See Figure 17.

If $\sum_k \psi_k > \sum_k \theta_k$ we use a slightly easier variant of the 420°-trick that we call the "120°-trick". This involves mapping a slit half-plane to a 120°-sector with a triangle removed, as shown in Figure 10. Traversing the boundary of the slit half-plane we encounter angles 60°, 360°, and 120°, but traversing the boundary of the modified 120°-sector we encounter 60°, 300° and 120°, so the ψ-sum decreases by 60° relative to the θ-sum. As in the 420°-trick, the shape of the slit can be chosen so that points on the two identified segments are paired according to their distance from the 300°-vertex. Then an equilateral triangulation of the modified sector maps to a triangulation of the half-plane. Note also that exactly one degree five vertex is created in the triangulation, located at the tip of the slit. See also Figure 14.

3 Conformal and quasiconformal maps

In this section we review the definition and basic properties of conformal and quasiconformal maps and state a number of specific estimates that are used to create and merge various triangulations. Detailed proofs of all lemmas and corollaries stated here are given in [8].

We let $D(z,r) = \{w : |z-w| < r\}$, $\mathbb{D} = D(0,1)$ and $\mathbb{T} = \partial\mathbb{D} = \{z : |z| = 1\}$. In this paper, a **conformal map** always refers to a 1-to-1 holomorphic mapping. Thus it is angle and orientation preserving. By the Riemann mapping theorem, there is a conformal map from $\mathbb{D}$ onto any proper, simply connected subdomain of the plane, in particular, the interior of any bounded polygon. The conformal map is unique if we specify the image of 0 and of one boundary point. For a conformal map onto the region Ω bounded by a N-gon P, the preimages of the N vertices are called the prevertices, and for an N-tuple of distinct points on $\mathbb{T}$.

The Riemann mapping theorem also holds for any simply connected Riemann surface that is not conformally

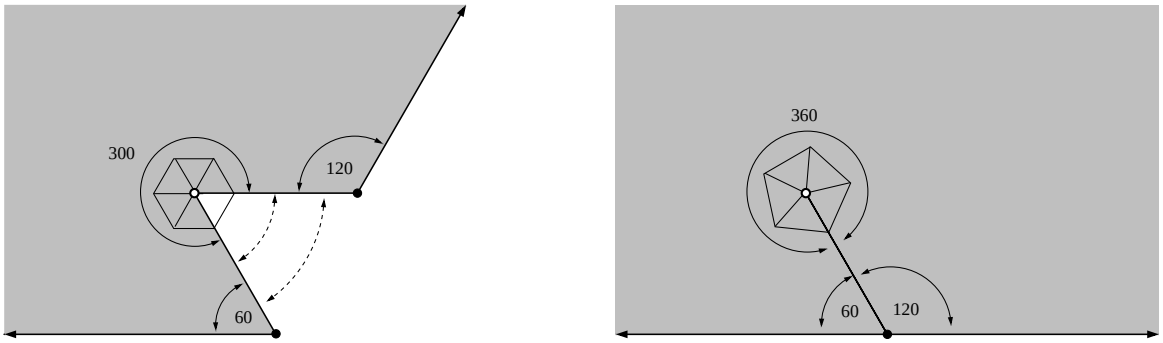

Figure 10: Take a 120°-sector and cut out an equilateral triangle (left). Conformally map this region to a slit half-plane (right). The two edges adjacent to the 300°-vertex are mapped to opposite sides of the (slightly) curved slit, and points on these edges equidistant from this vertex are identified. This implies that an equilateral triangulation on the left pushes forward to a triangulation on the right.

equivalent to the 2-sphere or the plane (this is usually called the uniformization theorem). All the Riemann surfaces that we will consider in this paper are simply connected and a have non-constant, holomorphic map into a bounded region of the plane; this implies they are conformally equivalent to the disk.

By definition, a conformal map f on a domain Ω preserves angles infinitesimally. When we map a triangulation by a conformal map, we will not just take the image $f(T)$ of each triangle T; this would have curved sides. If $T = \Delta ABC \subset \Omega$ has vertices A, B, C, we define the **pushed forward triangle** $f^*(T) = \Delta f(A)f(B)f(C)$, i.e., the triangle with vertices $f(A), f(B), f(C)$. See Figure 11.

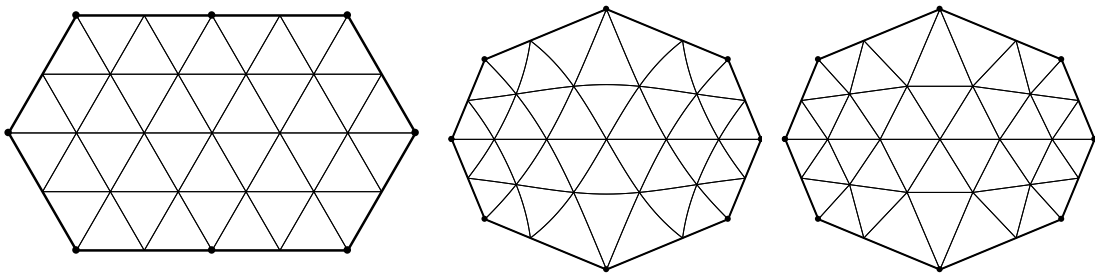

Figure 11: An equilateral triangulation (left), the actual conformal images of the triangles (center), and the pushed forward triangles (right) where vertex images are connected by segments.

LEMMA 3.1. *If f is a conformal map on a disk $D(z,r)$, $\delta > 0$ is sufficiently small, and $T = \Delta ABC$ is triangle inside $D(z,\delta r)$, then the triangle $f^*T = \Delta f(A)f(B)f(C)$ has angles that are within $O(\delta)$ of the corresponding angles of T.*

This result allows us to quantify the fact that, except near the corners, a conformal map between polygons alters the angles of small triangles very little under the push forward operation.

COROLLARY 3.1. *Suppose f is conformal map between the interiors of two polygons P and P' that maps vertices to vertices. Suppose V_P is the vertex set of P, Ω is the interior of P, and that $\{D_v\}_{v\in V_P}$ are disjoint disks around each vertex v. Define $\Omega_0 = \Omega \setminus \cup_{v\in V_P} D_v$ and suppose $T \subset \Omega_0$ is a triangle. Then for every $\epsilon > 0$ there is a $\delta > 0$ so that f changes the angles of T by less than ϵ if* $\operatorname{diam}(T) < \delta$.

An **infinite sector** is a region congruent to $S(\theta) = \{re^\phi : r > 0, -\theta/2 < \phi < \theta/2\}$. The boundary consists of two infinite rays meeting at its vertex and the angle of the sector is the interior angle θ made by these rays. A **finite sector** is a region congruent to $S(\theta) \cap D(0,t)$ for some $t > 0$ and $\theta \in (0, 360°]$. For $r > 1$, let $A(r) = \{z : 1/r < |z| < r\}$. An **annular sector** is a region congruent to $S(\theta, r) = S(\theta) \cap A(r)$.

LEMMA 3.2. *Suppose Ω_1, Ω_2 are simply connected domains and that both $\Omega_1 \cap A(3)$ and $\Omega_2 \cap A(3)$ have connected components equal to $S(\theta, 3)$. Suppose f_k is conformal on Ω_k, $k = 1, 2$ and $\sup_{S(\theta,3)} |f_1 - f_2| < \epsilon$. Suppose that f_1, f_2 both map each radial segment of $\partial S(\theta, 3)$ into the same line. Let $\eta : [0, \infty) \to [0, 1]$ be smooth with $\eta(r) = 0$ if $r < 1/2$ and $\eta(r) = 1$ if $r > 2$. Then*

$$g(z) = f_1(z)(1 - \eta(|z|)) + f_2(z)\eta(|z|)$$

is quasiconformal on $\Omega_1 \cup \Omega_2$ with complex dilatation bounded by $O(\epsilon)$.

A similar argument also proves the following slightly simpler variation, where we assume the maps are defined on a common disk, instead of a sector. This version will be used to merge triangulations near tips of slits in the 120°-trick (see Section 4) and the 420°-trick (see Section 5) .

LEMMA 3.3. *Suppose Ω_1, Ω_2 are simply connected domains and $D(0, r) \subset \Omega_1 \cap \Omega_2$ for some $r > 4$. Suppose $f : \Omega_1 \to \Omega_2$ is conformal and $f(0) = 0$, $f'(0) = 1$. Let $\eta : [0, \infty) \to [0, 1]$ be smooth with $\eta(r) = 0$ if $r \leq 1/2$ and $= 1$ if $r \geq 2$. Then*

$$g(z) = z(1 - \eta(|z|)) + f(z)\eta(|z|)$$

is quasiconformal on $\Omega_1 \cup \Omega_2$ with complex dilatation bounded by $O(1/r)$.

As noted in the introduction, not every 60°-polygon P has an equilateral triangulation, but in this section we will prove that they all have nearly equilateral triangulations. Recall that this means that for any $\epsilon > 0$, there is a triangulation of P with all angles within ϵ of 60° and that all angles are equal to 60° in some neighborhood of each vertex (the neighborhood may depend on the triangulation). Also recall that we need this result for both planar polygonal regions and Riemann surfaces with polygonal boundaries.

LEMMA 3.4. *Every 60°-surface P has nearly equilateral triangulations.*

Roughly speaking, the proof is to explicitly construct a 60°-surface R' that has an equilateral triangulation and that closely approximates R. Then show that the conformal map $R' \to \mathbb{D}$ can be composed with a quasiconformal map $\mathbb{D} \to \mathbb{D}$ with small dilatation, so that the vertices of R' map to the conformal prevertices of R on $\mathbb{T}$. From this we get a quasiconformal map $R' \to R$ that sends vertices to vertices and has small dilatation. Hence the equilateral triangulation of R' is pushed forward to a nearly equilateral triangulation of R (some extra work is needed to get true equilateral triangles near each vertex of R). For details see [8].

One step of the above lemma that we will need later is the following.

LEMMA 3.5. *Suppose $0 < \theta \leq 360°$ and that Ω_1, Ω_2 are simply connected domains such that $\Omega_1 \cap D(0, 1) = \Omega_2 \cap D(0, 1) = S(\theta) \cap D(0, 1)$ and f is a conformal map $\Omega_1 \to \Omega_2$ so that $f(0) = 0$. Then $f(z) = cz + O(z^2)$ on $D(0, 1/2)$ for some $c \neq 0$.*

Our last application of conformal mappings is to find good triangulations of infinite sectors; these will be used to triangulate a polygon near each of its vertices. As before, $S(\theta)$ denotes the infinite sector of angle θ with positive real half-line as its axis of symmetry. Note that $S(60°)$ comes with a natural equilateral triangulation $\mathcal{G}$ as shown in Figure 12. This triangulation can obviously be extended to a triangulation of the right half-plane, and our triangulations of general sectors are constructed by taking images of equilateral triangulations of special sectors (multiplies of 60°) under power maps $z \to z^\alpha$. See Figure 13 for two examples.

LEMMA 3.6. *Consider the grid $\mathcal{G}$ of unit equilateral triangles in $S(60°)$. Let $0 < \alpha \leq 2$. Suppose $T = \Delta ABC \in \mathcal{G}$ and $f^*T = \Delta f(A)f(B)f(C)$, where f is a branch of z^α defined on T. Then the interior angles of f^*T differ from the corresponding angles of T by at most $|\alpha - 1| \cdot \theta$ where θ is the angle subtended by T from the origin.*

COROLLARY 3.2. *Suppose $0 < \phi < 90°$. The sector $S(\phi)$ has a triangulation with all angles in $[180° - 2\phi, \phi]$ if $\phi \geq 60°$, and in $[\phi, 90° - \phi/2]$ if $\phi < 60°$.*

The sector triangulations described above are used in a neighborhood of each vertex of P. Outside these neighborhoods, the conformal image of a nearly equilateral triangulation is used. Quasiconformal interpolation is applied to merge the various triangulations in an annulus around each vertex. The precise statement of this procedure is given by the following lemma.

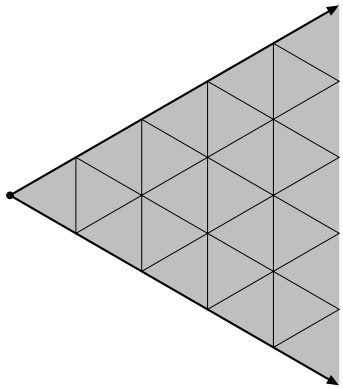

Figure 12: The sector $S(60°)$ and its equilateral triangulation $\mathcal{G}$.

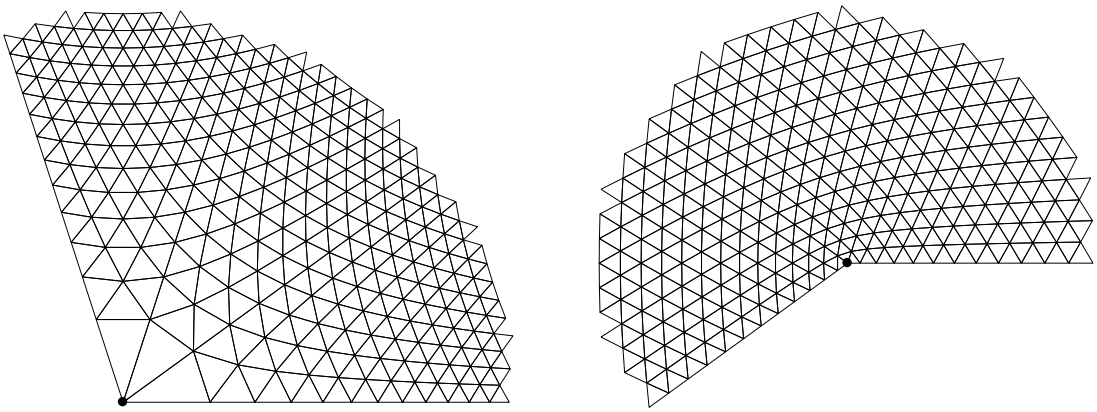

Figure 13: Image of the equilateral grid in the upper halfplane under the maps $z^{3/5}$ and $z^{6/5}$. These are the extreme values that keep images of 60° angles between 36° and 72°.

LEMMA 3.7. *Suppose $f : P' \to P$ is a conformal map between polygons that maps vertices to vertices. Suppose $f(v') = v$ where v' is a vertex of P' and v is a vertex of P, with angles $\psi = k \cdot 60°$ and θ respectively. Suppose $\mathcal{T}$ is a nearly equilateral triangulation of P' and $f^*\mathcal{T}$ the image triangulation. If $\mathcal{T}$ is fine enough, then there is a neighborhood U of v and a triangulation $\mathcal{S}$ of P that equals $f^*\mathcal{T}$ outside U and every triangle of $\mathcal{S}$ touching U has all angles bounded by* $\max(\theta/k, 90° - \theta/2k)$.

4 The 120°-trick

In this section we provide the details of the "120°-trick" for triangulating the upper half-plane in a way that uses maximum angle 72°, and near infinity looks like the push forward under $z^{3/2}$ of the standard equilateral mesh of a 120°-sector. This involves cutting a slit in P, as discussed in Sections 1 and 2.

Consider the region Ω shown on the left in Figure 10. This is a 120°-sector with an equilateral triangle at the origin removed. We translate the picture so the 300°-vertex is at the orgin. If we then apply a branch of $z^{6/5}$, the 300° angle becomes 360°, and the two finite segments in $\partial\Omega$ adjacent to it become identified with a radial slit in the image. The two rays in $\partial\Omega$ map to the boundary curve of a simply connected region Ω'. See lower left in Figure 14. By the Riemann mapping theorem, Ω' can be mapped to the upper half-plane, and the slit maps to a curved arc, meeting the real line at angle 60° (the slit looks quite straight since the tangents at the two endpoints differ by only $\approx 2.75°$).

Since the power map identifies points on the two segments adjacent to w that are equidistant from w, any equilateral triangulation of Ω will push forward to triangulation of the upper half-plane. If the triangulation is fine enough, then all the pushed forward triangles will be nearly equilateral, except near the corners and tip of

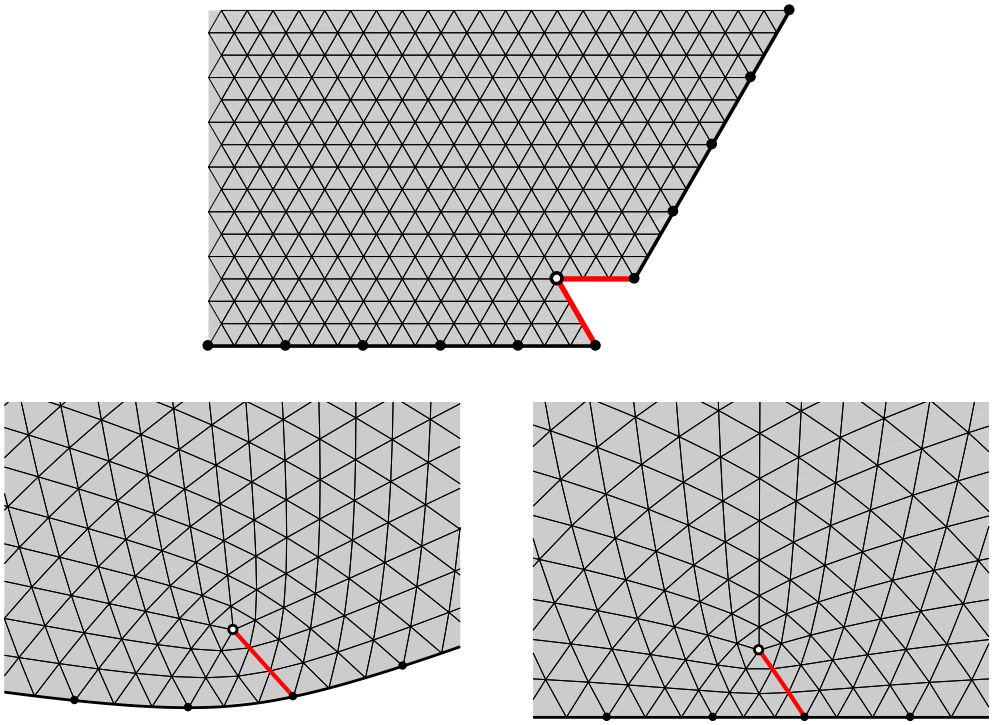

Figure 14: The cut 120-sector (top) is mapped to a simply connected region (lower left) by a branch of $z^{6/5}$. This is then mapped to the upper half-plane by a conformal map. Because the power map identifies points according to distance to zero (the white dot), the push forward of the triangulation is still a triangulation.

the slit. However, near the point v where the slit joins the real line, P looks like the union of a small 60°-sector and a 120°-sector and the map to P' sends each of these to subdomains of P' that contain and are contained in small sectors of the same angles. Thus by Lemma 3.5, the conformal maps restricted to each finite sector is approximately linear and the image of the equilateral triangulation of P' is close to equilateral in P near v. This leaves only the tip of slit. In a small neighborhood of the tip, angles are bounded above by $72° + \epsilon$ if the mesh is fine enough, but might exceed 72°. However, we can replace the mesh in a neighborhood of the tip by the standard mesh of a 360°-sector using Lemma 3.3. This gives the 72° bound. The construction is summarized in the the following lemma.

LEMMA 4.1. *Suppose $f : P' \to P$ is a conformal map between polygons that maps vertices to vertices. Suppose $f(v') = v$ where v' is a vertex of P' and v is a vertex of P, with angles* 120° *and* 180° *respectively. Suppose $\mathcal{T}$ is a nearly equilateral triangulation of P' and $f^*\mathcal{T}$ the image triangulation. If $\mathcal{T}$ is fine enough, then there is a neighborhood U of v and a triangulation $\mathcal{S}$ of P that equals $f^*\mathcal{T}$ outside U and every triangle of $\mathcal{S}$ touching U has all angles $\leq 72°$.*

5 The 420°-trick

There are two things we can do to increase the ψ-sum for P' by 60° with respect the θ-sum for P. The first is to introduce a 180°-vertex v in an edge of P and add a corresponding 240°-vertex v' to P'. This clearly increases the ψ-sum by an extra 60° relative to the θ-sum. The angle at v' is subdivided into four equilateral triangles by the nearly equilateral triangulation, and each of these are mapped to four angles of size 45° at v. The opposite angles in the image triangles are $67.5° < 72°$, so this construction will be enough for proving Case 1 of Theorem 1.1.

However, in order to handle Case 2 of Theorem 1.1 we need another "trick" that can add 60° to the ψ-sum relative to the θ-sum, but introduces triangulation angles no larger than $\frac{5}{7} \cdot 90° \approx 64.2857°$. This is precisely the

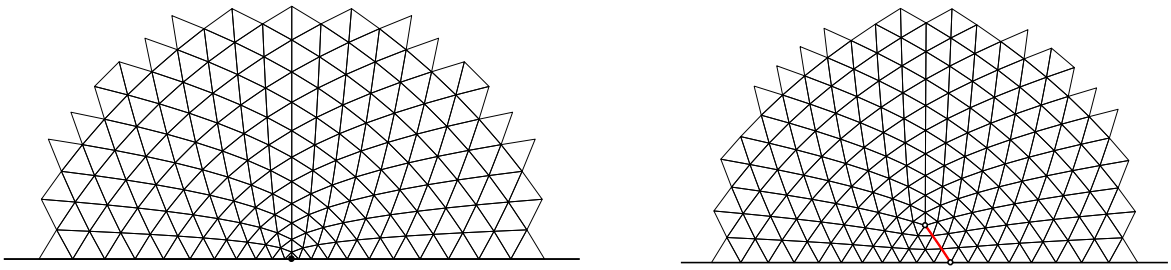

Figure 15: The left shows the equilateral triangulation of a 120°-sector pushed forward to the half-plane by $z^{3/2}$. The right shows the triangulation coming from the "120°-trick". These two meshes can be merged using quasiconformal interpolation as described in the text.

angle bound we get if a 420°-vertex $v' \in P'$ is mapped to a 360°-vertex $v \in P$. The 360° vertex v can occur as the end vertex of a slit in P, but how do we get a 420°-vertex in P'? We do this by considering a non-planar Riemann surface.

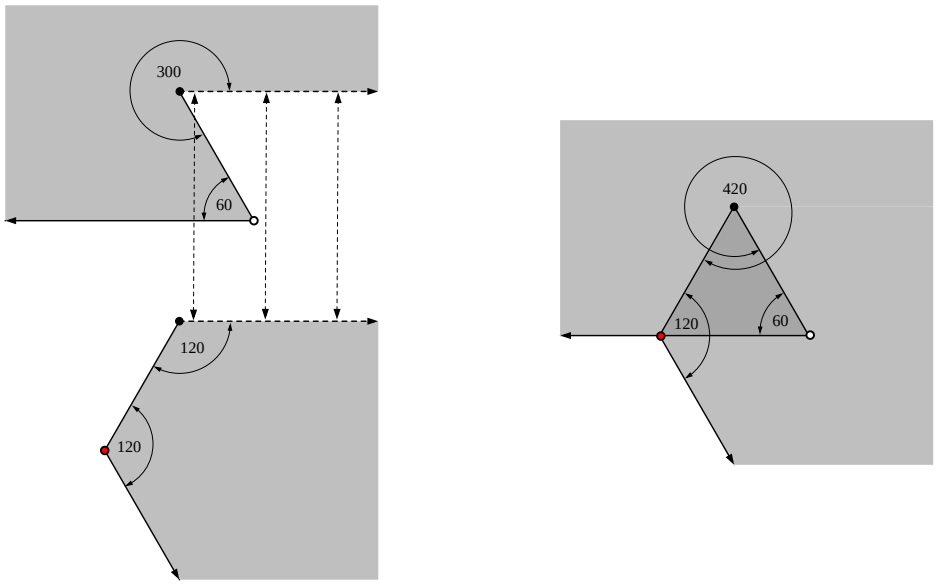

Figure 16: Here a 180° vertex in P corresponds to a 420° in P'. This is obtained by making P' a Riemann surface instead of a planar domain. The surface can be constructed from two planar domains glued along the dashed edges of each as illustrated on the left. The darker triangle indicates where the surface has two sheets over the plane.

The idea is illustrated in Figure 16. Consider the two planar regions shown on the left side of the figure and define a Riemann surface by identifying them along the dashed ray. This creates a simply connected Riemann surface R with single boundary curve that is the union of two infinite rays, two finite segments and has three corners of 60°, 420° and 120°.

We can conformally map R to a slit upper half-plane in two steps as illustrated in Figure 17 so that the two segments of ∂R that are adjacent to the 420° angle are identified with the slit, and length measure on these segments is pushed forward to the same measure on the slit. Translate the 420°-vertex to the origin and apply a branch of $z^{6/7}$ defined on R. This maps R to a simply connected planar domain Ω with a straight slit; the two segments of ∂R are identified with this slit in the correct way, and the two infinite rays are mapped to disjoint, unbounded arcs on $\partial\Omega$. The domain Ω can then be conformally mapped to a half-plane. Thus equilateral triangulations of R will be mapped to triangulations of the upper half-plane.

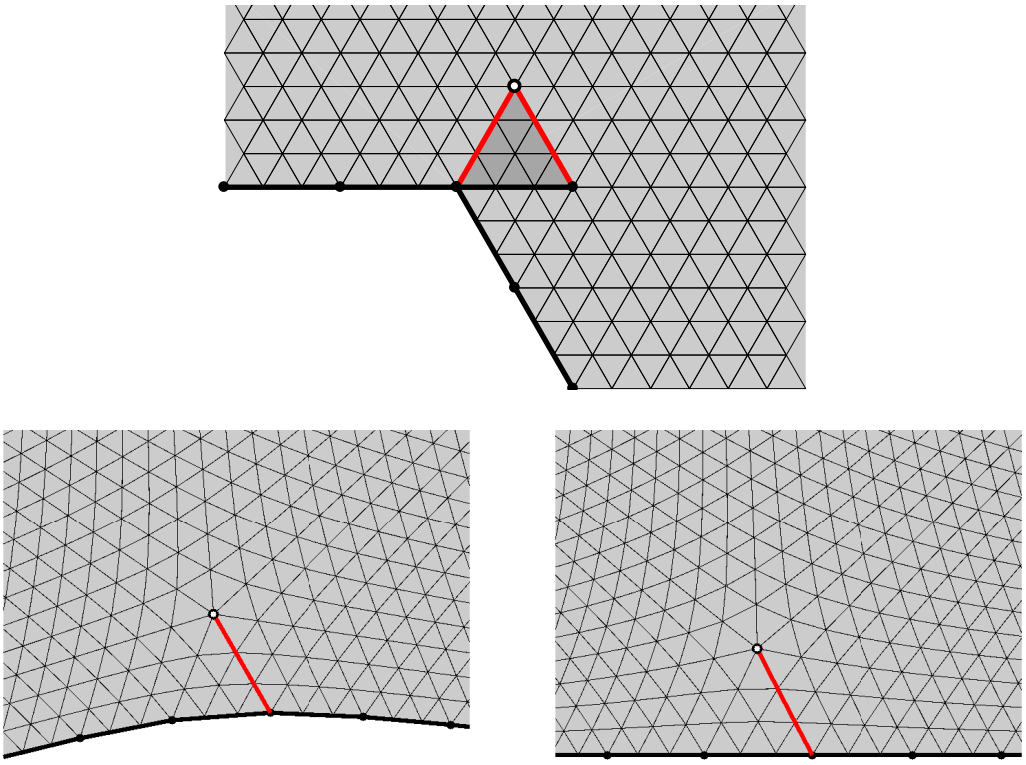

Figure 17: The Riemann surface R can be conformally mapped to a slit domain Ω by a branch of $z^{6/7}$. This map is followed by a conformal map to the upper half-plane that bends the the straight slit to an analytic arc (but it looks quite straight; the tangent directions only change by about 1° along the arc).

6 Sufficiency in Theorem 1.1

Necessity of the conditions in Theorem 1.1 was already sketched before the statement of the theorem, and more detailed arguments for this can be found in Gerver's paper [18] and in [8]. Here we prove the new direction of the theorem: sufficiency.

Proof. We want to show that any polygon P (possibly after adding extra vertices) can be conformally mapped to a 60°-polygon P', with the restrictions on the angles given by Table 1. We will use the 120°-trick to "fix" the pushed forward triangulation in a neighborhood of a few boundary points, but the 420°-trick is not needed until the proof of Cases 2 and 3 later.

The Schwarz-Christoffel formula gives a conformal map f of the disk onto a polygonal region P in terms of two types of data. First are the angles of P: suppose $V_P = \{v_j\}_1^N$ are the vertices of P and the interior angle at v_j is $\alpha_j \cdot 180°$. Second, suppose f maps $z_j \in \mathbb{T}$ to $v_j \in P$; these points are called the prevertices or Schwarz-Christoffel parameters of f. Then the conformal map f is given by

$$f(z) = A + C \int^z \prod_{j=1}^{N} (1 - \frac{w}{z_j})^{\alpha_j - 1} dw, \tag{6.3}$$

for some appropriate choice of constants A, C. See e.g., [13], [29], [35]. The formula was discovered independently by Christoffel in 1867 [10] and Schwarz in 1869 [34], [33]. For other references and a brief history, see Section 1.2 of [13]. Given a polygon P, the angles are known, but the prevertices must be solved for.

Given N distinct points $\mathbf{z} = \{z_1, \ldots, z_N\}$ on the unit circle and N real values $\{\alpha_1, \ldots, \alpha_N\}$ summing to $N-2$, Formula (6.3) defines a locally 1-1 holomorphic function on the disk that maps each component of $\mathbb{T} \setminus \mathbf{z}$ to a line segment, with the segments meeting at $f(z_k)$ making interior angle $\alpha_k \cdot 180°$. The map given by (6.3) is always locally 1-1 on $\mathbb{D}$, but need not be globally 1-1 in general. In this case, the image is a Riemann surface with an

obvious projection onto the plane. For the proof of Case 1 of Theorem 1.1 we can arrange for the image to be a planar 60°-polygon. In the proof of Cases 2 and 3, given at the end of this section, the image is allowed to be a non-planar 60°-surface (this occurs when we apply the 420° trick).

Given an N-gon P, we take some conformal map f of its interior to the unit disk, $\mathbb{D}$. The N vertices of P map to N distinct points $\mathbf{z} = \{z_1, \ldots, z_N\}$ on the unit circle $\mathbb{T}$. We then want to choose N real values $\psi_k \in Z = \{60°, 120°, 180°, 240°, 300°\}$ so that $\sum_k \psi_k = 180(N-2)$. If this is possible, we then set $\alpha_k = \psi_k/180$ and apply the Schwarz-Christoffel formula to get a map $g : \mathbb{D} \to P'$. Then $g \circ f : P \to P'$ is the desired map. However, as noted in Sections 1 and 2, such a choice of angles ψ_k may not be possible without adding extra vertices to P.

First choose six interior points of some edge of P. This creates an M-gon with $M = N + 6$. These are 180°-vertices in P and are assigned to have angle $\psi_v = 120°$ in P'. Assign angle 180° to every other vertex of P', so the ψ-angle sum is $6 \cdot 120° + 180°N = (M-2)180°$. Applying Schwarz-Christoffel gives a a 60°-hexagon, as in Figure 18.

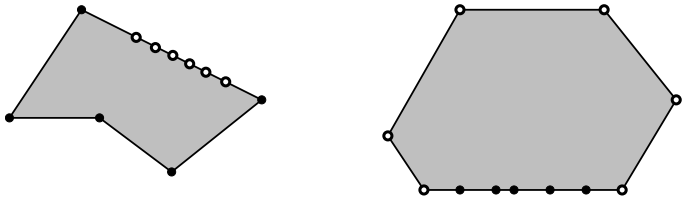

Figure 18: In the proof of Case 1 of Theorem 1.1 we can assume P' is planar. The first step is to choose six "artificial" vertices on one edge of P and make these correspond to six 120°-vertices in P'.

Next we modify the angle assignments to get a P' that approximates this hexagon. Let $L : V_P \to \mathbb{N}$ be a ϕ-admissible labeling of the vertices of P. For $v \in V_P$, assign angle $60° \cdot L(v)$ to the corresponding vertex v' of P'. In order to adjust the angle sums, for each vertex v of P we define either 0, 1 or 2 "associated vertices". The new vertices will be in the edge of P that begins with v (P has the counterclockwise orientation with the domain interior on the left) and may be taken as close to v as we wish. The vertices associated to v on P have angle 180° and the corresponding vertices associated to v' in P' have angle either 120° or 240°. These angles are assigned so that P' leaves the last associated vertex in the same direction as it entered v'. This implies that the part of P' near v' approximates a straight line. The rules for making the assignments are simple and illustrated in Figure 19. Suppose v is an original vertex of P with interior angle θ_v:

i. if $0 < \theta \leq 72°$, set $\psi_v = 60°$ and add two vertices each with angle 240°,

ii. if $72° < \theta \leq 144°$, set $\psi_v = 120°$ and add one vertex with angle 240°,

iii. if $144° < \theta \leq 216°$, set $\psi_v = 180°$ and add no associated vertices,

iv. if $216° < \theta \leq 288°$, set $\psi_v = 240°$ and add one vertex with angle 120°,

v. if $288° < \theta \leq 360°$, set $\psi_v = 300°$ and add two vertices of angle 120°.

If the vertices associated to v are close enough to v, then the image arc is close to a line. See Figure 20. In particular, P' is not self-intersecting and so is a 60°-polygon. By Lemma 3.4, P' has nearly equilateral triangulations. In the remainder of the proof we will take this triangulation as fine as is needed (but only finitely many conditions are involved, so we finish with a positive grid size).

Each original vertex with angle $\theta_v \geq 36°$ was assigned an image angle ψ_v in the allowable range from Table 1. Thus transferring a nearly equilateral triangulation of P' gives a triangulation of P with all angles between 36° and 72° except possibly in small neighborhoods of these vertices, where the angle bounds are with all angles between $36° - \epsilon$ and $72° + \epsilon$, and ϵ can be made as small as we wish be taking the triangulation fine enough. In a neighborhood of each such vertex, we may use Lemma 3.7 to replace the pushed forward triangulation with a sector triangulation for which the bounds $36°, 72°$ hold.

For each original vertex with interior angle $\theta_v < 36°$ the same argument applies, except that now we get the bounds in the interval $I(\theta_v) = [\theta_v, 90° - \theta_v/2]$. Again, we may use interpolation to locally replace the pulled

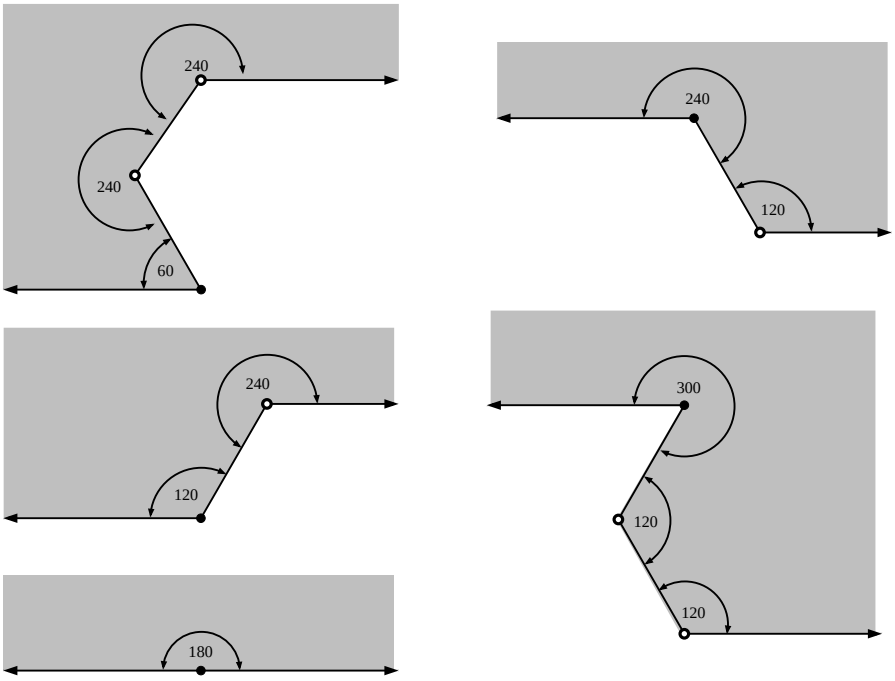

Figure 19: The five cases for assigning image angles and associated vertices. In each case the black indicates the image of the original vertex and the white dots the new associated vertices. These arcs illustrate small subarcs of the 60°-polygon P'. The associated vertices map to 180° vertices that we add to the edges of P.

back triangulation (which might only approach the desired bounds as the triangulation gets finer), with a sector triangulation satisfying the desired bounds.

Next consider the associated vertices with angles $> 120°$; Cases (i) and (ii) above. In Case (i) each 240°-vertex is hit by 4 equilateral triangles and so each 60° sub-angle is mapped to an angle of size $180°/4 = 45°$. In this case, the interpolation with a sector triangulation isn't needed; with small enough distortion, the angles are already inside $[36°, 72°]$. Case (ii) is the same, except there is only one associated vertex.

Finally we consider Cases (iv) and (v). Here we only use image angles of size 120°. Such an angle is divided into two 60° angles that are mapped to 90° by the conformal map: too large. We use Lemma 4.1 to interpolate between the conformal image triangulation and the triangulation of the half-plane coming from the 120°-trick. This gives a triangulation of with angles in $I(36°) = [36°, 72°]$ in a neighborhood of each associated vertex. This completes the proof of Case 1 of Theorem 1.1.

We turn to the other two cases. We just have to modify the construction in the proof of Case 1 to avoid using the 120°-trick in Case 2 (this forces an angle $\geq 72°$), and to avoid both the 120°-trick and the 420°-trick in Case 3 (the latter forces angles $\geq \frac{5}{7} \cdot 90°$).

Suppose L is a ϕ-admissible labeling of V_P so that $\kappa(\phi) = \kappa(L)$ (i.e., choose L to minimize $|\kappa(L)|$ among admissible labelings). As before, let θ_v denote the angle of P at vertex v, and for each vertex v in P, suppose $\psi_v = L(v) \cdot 60°$ is the tentative corresponding angle of v' in P'. As we have noted before,

$$\begin{aligned} \sum_v \theta_v &= (|V_P| - 2)180° = 60°(3|V_P| - 6) \\ &= 60° \left(3|V_P| - 6 - \sum_v L(v) + \sum_v L(v) \right) = 60° \cdot \kappa(L) + \sum_v \psi_v. \end{aligned}$$

Thus in Case 2 ($\kappa(L) \leq 0$) we only need to introduce 180°-vertices on P that correspond to 240°-vertices in P'. If $\phi \geq 67.5°$, we can do this by replacing the pushed forward triangulation from P' by the 240°-sector triangulation. If $\frac{5}{7} \cdot 90° \leq \phi < 67.5°$ then we replace it with the triangulation of the half-plane obtained by the 420°-trick. This proves sufficiency in Case 2.

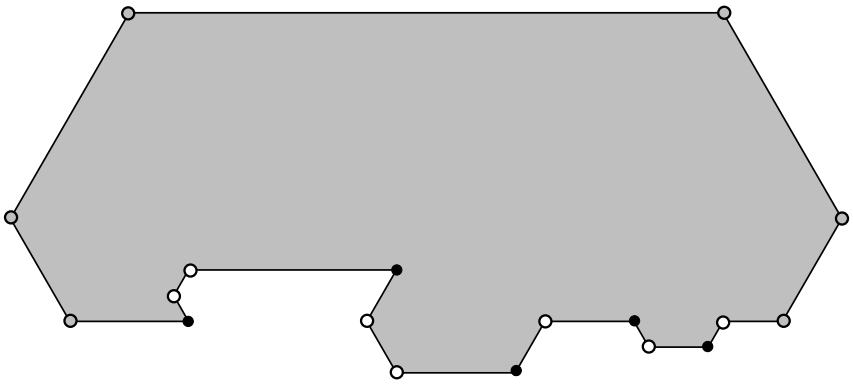

Figure 20: The 60°-polygon P'. The six gray points were added at the beginning, the black points are the images of the original vertices and the white points are the associated vertices.

Finally, if $\kappa(L) = 0$, then no extra vertices or "tricks" are needed. We simply use a fine enough triangulation pushed forward by the conformal map from P' to P and replace it in a neighborhood of each vertex by the appropriate sector mesh. This completes the proof in Case 3. □

References

[1] B.S. Baker, E. Grosse, and C.S. Rafferty. Nonobtuse triangulation of polygons. *Discrete Comput. Geom.*, 3(2):147–168, 1988.

[2] M. Bern, H. Edelsbrunner, D. Eppstein, S. Mitchell, and T. S. Tan. Edge insertion for optimal triangulations. In *LATIN '92 (São Paulo, 1992)*, volume 583 of *Lecture Notes in Comput. Sci.*, pages 46–60. Springer, Berlin, 1992.

[3] M. Bern, D. Eppstein, and J. Gilbert. Provably good mesh generation. *J. Comput. System Sci.*, 48(3):384–409, 1994. 31st Annual Symposium on Foundations of Computer Science (FOCS) (St. Louis, MO, 1990).

[4] M. Bern, S. Mitchell, and J. Ruppert. Linear-size nonobtuse triangulation of polygons. *Discrete Comput. Geom.*, 14(4):411–428, 1995. ACM Symposium on Computational Geometry (Stony Brook, NY, 1994).

[5] M. Bern and P. Plassmann. Mesh generation. In *Handbook of computational geometry*, pages 291–332. North-Holland, Amsterdam, 2000.

[6] C. J. Bishop. Conformal welding and Koebe's theorem. *Ann. of Math. (2)*, 166(3):613–656, 2007.

[7] C.J. Bishop. Nonobtuse triangulations of PSLGs. *Discrete Comput. Geom.*, 56(1):43–92, 2016.

[8] C.J. Bishop. Optimal triangulation of polygons. 2021. Preprint.

[9] Yu. D. Burago and V. A. Zalgaller. Polyhedral embedding of a net. *Vestnik Leningrad. Univ.*, 15(7):66–80, 1960.

[10] E.B. Christoffel. Sul problema della tempurature stazonaire e la rappresetazione di una data superficie. *Ann. Mat. Pura Appl. Serie II*, pages 89–103, 1867.

[11] H.T. Croft, K.J. Falconer, and R.K. Guy. *Unsolved problems in geometry*. Problem Books in Mathematics. Springer-Verlag, New York, 1991.

[12] T.A Driscoll. Algorithm 843: Improvements to the Schwarz-Christoffel Toolbox for MATLAB. *ACM Transactions on Mathematical Software (TOMS)*, 31(2):239–251, 2005.

[13] T.A. Driscoll and L.N. Trefethen. *Schwarz-Christoffel mapping*, volume 8 of *Cambridge Monographs on Applied and Computational Mathematics*. Cambridge University Press, Cambridge, 2002.

[14] H. Edelsbrunner. Triangulations and meshes in computational geometry. In *Acta Numerica, 2000*, volume 9 of *Acta Numer.*, pages 133–213. Cambridge Univ. Press, Cambridge, 2000.

[15] H. Edelsbrunner, T.S. Tan, and R. Waupotitsch. An $O(n^2 \log n)$ time algorithm for the minmax angle triangulation. *SIAM J. Sci. Statist. Comput.*, 13(4):994–1008, 1992.

[16] D. Eppstein. Acute square triangulation. Webpage https://www.ics.uci.edu/ eppstein/junkyard/acute-square/, Accessed: January 2, 2021.

[17] H. Erten and A. Üngör. Computing acute and non-obtuse triangulations. In *CCCG 2007, Ottawa, Cananda*. 2007.

[18] J. L. Gerver. The dissection of a polygon into nearly equilateral triangles. *Geom. Dedicata*, 16(1):93–106, 1984.

[19] J.E. Goodman, J. O'Rourke, and C.D. Tóth, editors. *Handbook of discrete and computational geometry*. Discrete Mathematics and its Applications (Boca Raton). CRC Press, Boca Raton, FL, 2018. Third edition of [MR1730156].

[20] D. H. Hamilton. Conformal welding. In *Handbook of complex analysis: geometric function theory, Vol. 1*, pages 137–146. North-Holland, Amsterdam, 2002.
[21] J. Itoh and T. Zamfirescu. Acute triangulations of the regular icosahedral surface. *Discrete Comput. Geom.*, 31(2):197–206, 2004.
[22] S. Korotov and J. Stańdo. Nonstandard nonobtuse refinements of planar triangulations. In *Conjugate gradient algorithms and finite element methods*, Sci. Comput., pages 149–160. Springer, Berlin, 2004.
[23] C.L. Lawson. *Software for C^1 surface interpolation*, pages ix+388. Academic Press [Harcourt Brace Jovanovich Publishers], New York, 1977. Publication of the Mathematics Research Center, No. 39.
[24] D. T. Lee and A. K. Lin. Generalized Delaunay triangulation for planar graphs. *Discrete Comput. Geom.*, 1(3):201–217, 1986.
[25] J. Y. S. Li and H. Zhang. Nonobtuse remeshing and mesh decimation. In *SGP '06: Proceedings of the fourth Eurographics symposium on Geometry processing*, pages 235–238, Aire-la-Ville, Switzerland, Switzerland, 2006. Eurographics Association.
[26] H. Maehara. Acute triangulations of polygons. *European J. Combin.*, 23(1):45–55, 2002.
[27] E.A. Melissaratos and D.L. Souvaine. Coping with inconsistencies: a new approach to produce quality triangulations of polygonal domains with holes. In *SCG '92: Proceedings of the eighth annual symposium on computational geometry*, pages 202–211, New York, NY, USA, 1992. ACM.
[28] S.A. Mitchell. Approximating the maxmin-angle covering triangulation. volume 7, pages 93–111. 1997. Fifth Canadian Conference on Computational Geometry (Waterloo, ON, 1993).
[29] Z. Nehari. *Conformal mapping*. Dover Publications Inc., New York, 1975. Reprinting of the 1952 edition.
[30] S. Rohde. On conformal welding and quasicircles. *Michigan Math. J.*, 38:111–116, 1991.
[31] J. Ruppert. A new and simple algorithm for quality 2-dimensional mesh generation. In *Proceedings of the Fourth Annual ACM-SIAM Symposium on Discrete Algorithms (Austin, TX, 1993)*, pages 83–92, New York, 1993. ACM.
[32] S. Saraf. Acute and nonobtuse triangulations of polyhedral surfaces. *European J. Combin.*, 30(4):833–840, 2009.
[33] H.A. Schwarz. Confome abbildung der oberfläche eines tetraeders auf die oberfläche einer kugel. *J. Reine Ange. Math.*, pages 121–136, 1869. Also in collected works, [34], pp. 84-101.
[34] H.A. Schwarz. *Gesammelte Mathematische Abhandlungen*. Springer, Berlin, 1890.
[35] L. N. Trefethen and T.A. Driscoll. Schwarz-Christoffel mapping in the computer era. In *Proceedings of the International Congress of Mathematicians, Vol. III (Berlin, 1998)*, number Extra Vol. III, pages 533–542 (electronic), 1998.
[36] L.N. Trefethen. Numerical computation of the Schwarz-Christoffel transformation. *SIAM J. Sci. Statist. Comput.*, 1(1):82–102, 1980.
[37] L. Yuan. Acute triangulations of polygons. *Discrete Comput. Geom.*, 34(4):697–706, 2005.
[38] C.T. Zamfirescu. Survey of two-dimensional acute triangulations. *Discrete Math.*, 313(1):35–49, 2013.

C.J. Bishop, Dept. of Math., Stony Brook University, Stony Brook NY 11794-3651
bishop@math.stonybrook.edu